WILLIAM LETTIS & ASSOCIATES, INC.

Final Technical Report

Initial Evaluation of Paleoearthquake Timing On the Northern San Andreas Fault At the Fort Ross Orchard Site, Sonoma County, California

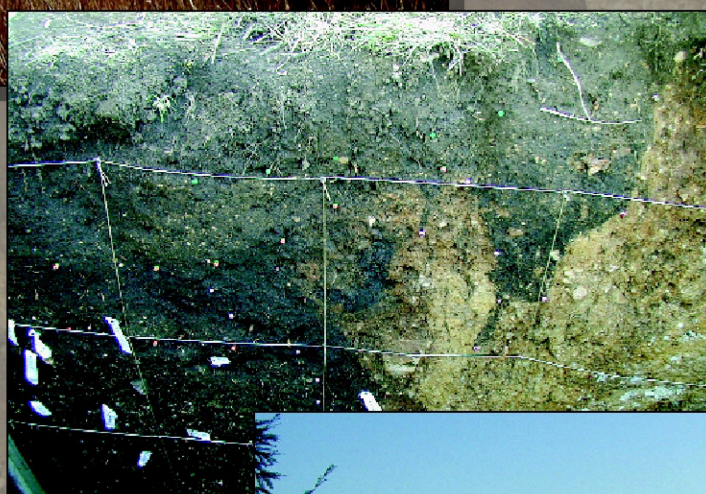

William Lettis & Associates, Inc.
1777 Botelho Dr., Suite 262
Walnut Creek, CA 94596

Principal Investigators:

Keith I. Kelson, Rich D. Koehler,
and Keng-Hao Kang

U.S. Geological Survey
National Earthquake Hazard Reduction Program
Award Number 00-HQ-GR-0072

September 2003

FINAL TECHNICAL REPORT

INITIAL EVALUATION OF PALEOEARTHQUAKE TIMING ON THE NORTHERN SAN ANDREAS FAULT AT THE FORT ROSS ORCHARD SITE, SONOMA COUNTY, CALIFORNIA

Recipient:

William Lettis & Associates, Inc.
1777 Botelho Dr., Suite 262, Walnut Creek, CA 94596
Phone: (925) 256-6070; Fax: (925) 256-6076

Principal Investigators:

Keith I. Kelson, Rich D. Koehler, and Keng-Hao Kang
Email: kelson@lettis.com

Program Element II
Paleoseismology, Trench Investigations, Quaternary Fault Behavior

U. S. Geological Survey
National Earthquake Hazards Reduction Program
Award Number 00-HQ-GR-0072

September 2003

Research supported by the U.S. Geological Survey (USGS), Department of the Interior, under USGS award number (William Lettis & Associates, Inc., 01-HQ-GR-0072). The views and conclusions contained in this document are those of the authors and should not be interpreted as necessarily representing the official policies, either expressed or implied, of the U.S. Government.

Award No. 00-HQ-GR-0072

INITIAL EVALUATION OF PALEOEARTHQUAKE TIMING ON THE NORTHERN SAN ANDREAS FAULT AT THE FORT ROSS ORCHARD SITE, SONOMA COUNTY, CALIFORNIA

Keith I. Kelson, Rich D. Koehler, and Keng-Hao Kang
William Lettis & Associates, Inc.
1777 Botelho Dr., Suite 262, Walnut Creek, CA 94596
Phone: (925) 256-6070; Fax (925) 256-6076
kelson@lettis.com

ABSTRACT

The Fort Ross Orchard site, which lies astride the North Coast segment of the San Andreas Fault, is characterized by a narrow, linear shutter ridge and associated linear trough within which latest Holocene sediments have accumulated. We excavated one trench across the San Andreas Fault and into these alluvial sediments, and one fault-parallel trench northeast of the fault to provide three-dimensional exposures of the alluvium trapped behind the linear ridge. We excavated a third intersecting trench, also parallel to the fault, along the crest of a linear ridge southwest of the fault, in order to expose a buried paleochannel that traverses the ridge crest. We interpret that this paleochannel is the southwestern extension of the present-day incised drainage northeast of the fault that is the source of the trapped alluvium.

In general, the trenches show that the alluvial-fan sediments consist of clayey sand that are as old as about AD 230, with only the uppermost, post-1906 deposits being undeformed by the fault. The trench exposures also show the presence of scarp-derived colluvium shed into the linear depression from the bedrock-cored shutter ridge. This colluvium grades into the uppermost alluvial units in the linear depression. We interpret that the colluvium reflects degradation of the scarp produced during the 1906 surface rupture at the site.

Geologic relations exposed in the cross-fault trench at the Fort Ross Orchard site provide possible evidence of three pre-1906 earthquakes, although all of the evidence is equivocal at this time. Beneath the post-1906 colluvium is a sheared deposit that may be either faulted alluvium or an older fissure fill. Stratigraphic relations, age dating, and the presence of possible shearing suggest that this unit is younger than about AD 1640 but older than AD 1906. Two pre-1640 earthquakes are suggested by two upward fault terminations within the lower alluvium, although both of these terminations occur at different stratigraphic levels. Given the available deposit age-estimates, the trench relations suggest possible surface ruptures between AD 230 and 1290, between AD 780 and 1640, and between AD 1640 and 1906. We emphasize that these data are poorly constrained, and that additional exposures of faulted deposits and additional age dates are needed to confirm or refute any of these possible ruptures. Nevertheless, the broad time

windows for these speculative ruptures are consistent with other nearby sites on the North Coast segment of the San Andreas Fault.

Our excavations at the Fort Ross Orchard site also included fault-parallel trenches on both sides of the fault to provide possible stratigraphic constraints on fault slip rate. One trench excavated across a topographic saddle along the crest of the linear ridge west of the fault exposed a 1-m-wide sediment-filled bedrock paleochannel that trends roughly orthogonal to the fault. Based on multiple age dates from charcoal in this paleochannel, we interpret an age of AD 1260 to 1390 for the deposits filling the paleochannel, although a broad range in age-dates allows the channel to be considerably older. We excavated a third trench on the eastern side of the fault to test the hypothesis that the paleochannel originally was a through-going channel that has been offset and thus can be used as a piercing point to estimate the late Holocene fault slip rate. Unfortunately, a similar paleochannel was not encountered in the fault-parallel trench northeast of the fault, and the available trench exposures did not provide well-constrained information on the fault slip rate.

Nevertheless, this field effort provides information that may help limit the late Holocene slip rate on the San Andreas Fault at this site. We speculate that the trench northeast of the fault was not long enough to expose the paleochannel on this side of the fault. Based on our detailed field survey of the site, the minimum amount of fault offset of the paleochannel, if present, is 17 m. These data suggest a minimum late Holocene slip rate of 25 mm/yr, which is notably higher than the rate of 19 $\pm$ 4 mm/yr obtained by recent studies at the nearby sites. Because we find no viable stratigraphic or geomorphologic explanation for the absence of the paleochannel northeast of the fault, we speculate that our age estimate for the paleochannel may be too young. Thus, although the data developed in this study suggests a minimum slip rate of 25 mm/yr for the San Andreas Fault, the uncertainty in deposit age suggests that this rate is not robust.

TABLE OF CONTENTS

Section — Page

ABSTRACT i
TABLE OF CONTENTS iii
1.0 INTRODUCTION 1
2.0 GEOLOGIC SETTING OF THE FORT ROSS ORCHARD SITE 3
  2.1 Description of the Fort Ross Orchard Site 3
3.0 PALEOSEISMIC RESULTS 9
  3.1 Trench Stratigraphy 9
    3.1.1 Age Estimates 15
    3.1.2 Stratigraphic Interpretation 18
  3.2 Trench Geologic Structure 19
4.0 INTERPRETATION AND DISCUSSION 21
5.0 CONCLUSIONS 24
6.0 ACKNOWLEDGEMENTS 26
7.0 REFERENCES 27

LIST OF FIGURES

Page

Figure 1 Regional Map of the San Andreas Fault 2
Figure 2 Location of Paleoseismic Sites Along the San Andreas Fault Near Fort Ross 4
Figure 3 Enlarged fault map of Brown and Wolf (1972) of the Fort Ross Orchard Site 6
Figure 4 Detailed Topographic Map of the Fort Ross Orchard Site 7
Figure 5a Log of Trench 1 10
Figure 5b Lithologic Descriptions of Units in Trenches 1, 2, and 3 11
Figure 6 Log of Trench 2 12
Figure 7 Log of Trench 3 13

LIST OF TABLES

Page

Table 1 Summary of Radiocarbon Ages, Fort Ross Orchard Site 17

1.0
INTRODUCTION

The primary goal of this investigation of the northern San Andreas Fault at the Fort Ross Orchard site is to provide information on the late Holocene paleoseismic history of surface-rupture earthquakes. Data on the timing of past events are essential for evaluating rupture segmentation of the northern San Andreas Fault and for estimating the probability and size of future earthquakes on the fault. In addition, understanding the timing of past large earthquakes along the northern San Andreas Fault is critical to estimating probabilities of future earthquakes in the San Francisco Bay region (Working Group on California Earthquake Probabilities [WGCEP], 2003).

The great San Francisco earthquake of 1906 produced surface rupture from San Juan Bautista to Cape Mendocino (Lawson, 1908; Thatcher and others, 1997; Prentice and others, 1999) (Figure 1). The North Coast segment of the San Andreas Fault that ruptured in 1906 currently is aseismic or nearly so (Hill and others, 1990). Previous workers have interpreted this relative lack of seismicity as evidence that the fault is "locked", and actively storing elastic strain energy for release in a future large-magnitude earthquake. The history of earthquakes along the North Coast segment is a critical element for probabilistic hazard assessments for the San Francisco Bay area. The WGCEP (1990) assumed that the North Coast segment ruptures as a single segment, mainly because of a lack of data suggesting otherwise. However, later work by the WGCEP (1999, 2003) considered several alternative rupture models, including a model in which the North Coast segment always ruptures in 1906-type events and models in which the North Coast segment contains sub-segments that rupture in smaller magnitude ($M_W \leq 6.9$) earthquakes. These different models have significant implications for the recurrence of various magnitudes of earthquakes, and thus for the probabilities of earthquakes along this section of the fault. The WGCEP (2003) rupture models and weightings reflect a consensus view that the fundamental behavior of the San Andreas Fault is expressed as full-length ruptures similar to the 1906 earthquake, with lesser likelihoods of smaller segment ruptures.

Thatcher and others (1997) used geodetic measurements to resolve coseismic fault slip along the entire 470-km-long rupture of the 1906 earthquake (Figure 1). Variations in amount of geodetic slip along the fault estimated by these workers are similar to observed variations in surface offsets (i.e., offset fences, tree lines) documented by Lawson (1908). Geodetic and surface measurements suggest a smaller amount of slip in the Fort Ross area than elsewhere along the North Coast segment (Figure 1). This is particularly relevant to interpretations of rupture segmentation of the San Andreas Fault. If the North Coast segment typically ruptures in 1906-type events, with similar distributions of coseismic slip along the fault, then a “slip deficit” would develop in the Fort Ross area (Schwartz and others, 1998). In this scenario, additional smaller magnitude (e.g., $M_W \leq 6.9$) earthquakes would be required near Fort Ross, in order to satisfy the long-term slip budget of the fault. The WGCEP (2003) considered the possibility of a smaller earthquake in the Fort Ross area through inclusion of a floating, M_W 6.9 earthquake anywhere along the 470-km-long segment that ruptured in 1906.

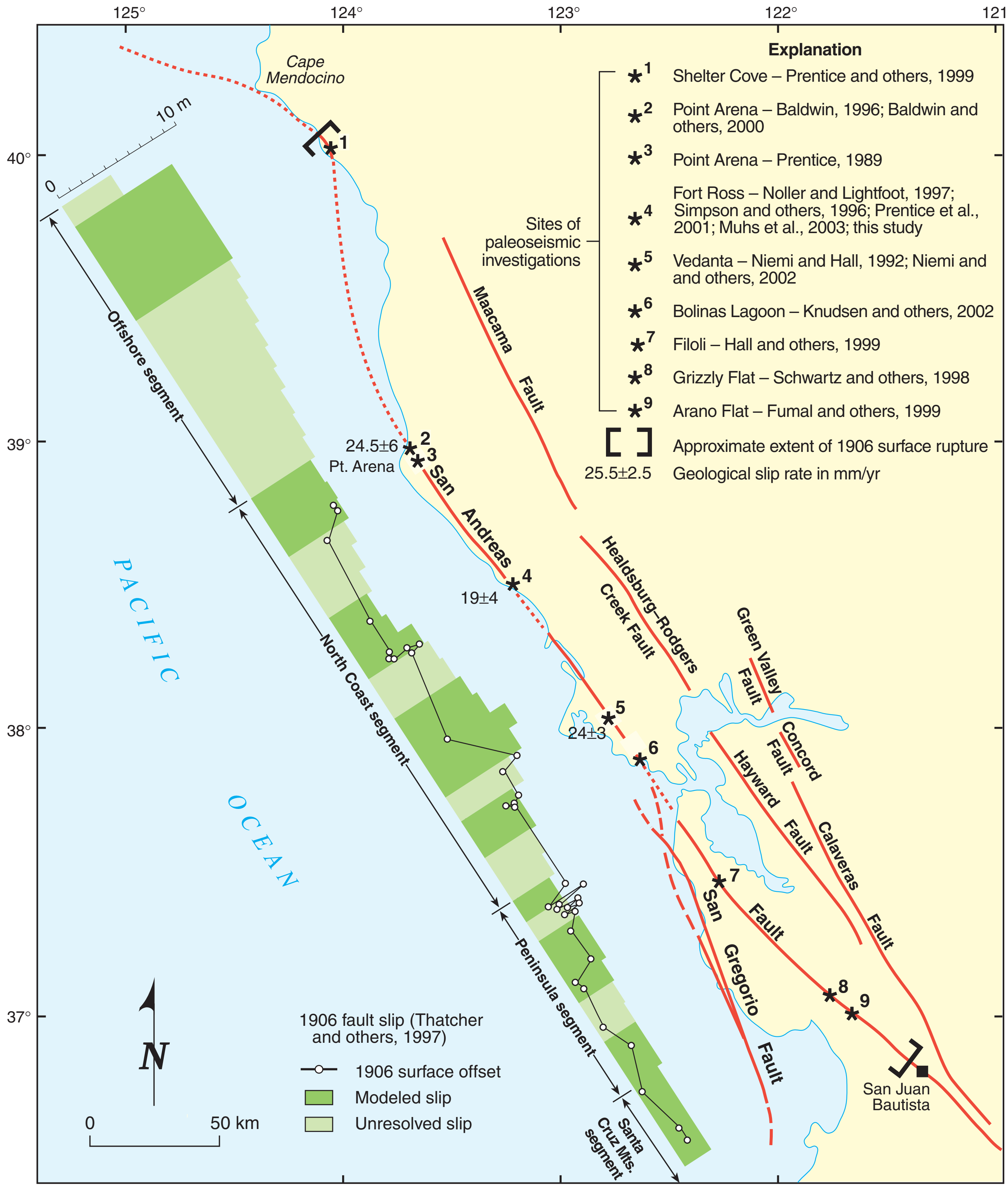

Figure 1. Regional map of the San Andreas Fault in northern California, showing location of 1906 rupture, fault segments from WGCEP (2003), previous paleoseismic sites, and the distribution of surface and geodetic slip produced by the 1906 rupture (Thatcher et al., 1997).

2.0

GEOLOGIC SETTING OF THE FORT ROSS ORCHARD SITE

The Fort Ross Orchard site lies along the North Coast segment of the San Andreas Fault, as defined most recently by the WGCEP (2003). This 191-km-long segment extends from Point Arena on the north to a complex intersection with the San Gregorio Fault in the offshore area west of the Golden Gate (WGCEP, 2003; Figure 1). This is the longest of four segments interpreted along the 470-km-long section of the San Andreas Fault that ruptured in 1906. Surface observations and geodetic modeling indicate that the part of the North Coast segment between Point Arena and Fort Ross experienced a lower amount of slip during the 1906 earthquake than other parts of the rupture (Lawson, 1908; Thatcher et al., 1997). Paleoseismic investigations at Point Arena (Prentice, 1989) and Olema (Niemi and Hall, 1992) suggest geologic slip rates of 23 ± 3 mm/yr and 24 ± 3 mm/yr, respectively, although studies near Fort Ross (Noller et al., 1993; Noller and Lightfoot, 1997; Prentice et al., 2001) suggest a preliminary rate of 19 ± 4 mm/yr. The recurrence of past earthquakes on the North Coast segment is estimated from the occurrence of at least five surface-rupturing earthquakes during the past 2000 years near Point Arena (Prentice, 1989), and the occurrence of at least seven surface ruptures within the past 2,000 to 2,500 years at Vedanta (Figure 1; Niemi et al., 2002). Knudsen et al. (2001) interpret geologic evidence to indicate the occurrence of three events within the past thousand years or so at Bolinas Lagoon (Figure 1). Collectively, these studies indicate a range in recurrence for large earthquakes on the North Coast segment of the San Andreas Fault of 180 to 370 years (WGCEP, 2003).

2.1 Description of the Fort Ross Orchard Site

The Fort Ross Orchard site is about 1.0 km northwest of the Archae Camp site, where we trenched in 1993 and 1994 (Noller and others, 1993; Simpson and others, 1996; Noller and Lightfoot, 1997), and about 2.8 km northwest of the Mill Gulch site investigated by Prentice et al. (2000, 2001). The San Andreas Fault between Fort Ross and Point Arena forms the boundary between the Gualala structural block on the southwest and the uplifted Coast Ranges on the northeast. The southernmost part of the Gualala block near Fort Ross contains discontinuous remnants of emergent marine terraces (Prentice, 1989), which may yield additional information on the pattern of deformation in this area (Muhs et al., 2003). The San Andreas Fault in the vicinity of Fort Ross is associated with prominent geomorphic features, including side-hill benches, sag ponds, linear drainages, shutter ridges, and uphill-facing scarps (Brown and Wolfe, 1972; Figure 2). Numerous cultural features were offset along the fault during the 1906 earthquake, including Fort Ross Road, an unnamed ranch road 150 m southeast of the Fort Ross Orchard site, and a fence presently marking the southeastern border of Fort Ross State Historic Park (Figure 2). Matthes (in Lawson, 1908) noted that Fort Ross Road was offset about 2.3 m (7.5 ft) and the ranch road and fence both were offset about 3.6 m (12 ft). The lower amount of measured offset of Fort Ross Road may be related to the presence of a secondary fault strand that joins the main strand in the vicinity of the Fort Ross Orchard site (Figure 2).

The Fort Ross Orchard site was chosen for investigation because it has (1) excellent geomorphic relations that constrain the location of the main strand of the fault, (2) late Holocene deposits in a

Figure 2. Location of paleoseismic sites along the San Andreas Fault near Fort Ross. The Fort Ross Creek site is a site that is planned for investigation in 2003 (Kelson and Lettis, in preparation).

depositional basin formed by an uphill-facing scarp, (3) minimal cultural disturbance, and (4) amenable landowners. The site includes a prominent, northwest-trending linear shutter ridge, uphill-facing scarp, and linear depressions that clearly mark the location of the main strand of the San Andreas Fault (Figure 3). The linear ridge traversing the site acts as a buttress for alluvial-fan sediment derived from a small, incised drainage gulley northeast of the site (Figure 4). Based on our field reconnaissance of the San Andreas Fault near Fort Ross, we viewed this site as one of the most promising sites for obtaining information on the late Holocene history of the North Coast segment of the fault. In addition, the site is within the Fort Ross State Historic Park, and thus we were able to obtain permission to conduct the investigation.

In a general sense, the Fort Ross Orchard site is situated on the southwest-facing front of the high-relief Coast Ranges (Figure 2). Southwest of the Fort Ross Orchard site, the Gualala block is associated with remnants of at least three emergent marine terraces, which form a stepped topography between the site and the Pacific coastline (Figure 2). Several steep-walled ravines are incised into the Gualala block, including Kollmer Gulch northwest of the Fort Ross Orchard site, Fort Ross Creek and Mill Gulch southeast of the site, and several tributaries to these streams (Figure 2). Locally, the San Andreas Fault lies within northwest-trending sections of these ravines, which have steep valley walls and dense vegetation. The areas between the major incised ravines generally are characterized by rolling topography strongly affected by surface fault deformation and/or landsliding. Previous paleoseismic sites in the Fort Ross area have been located in these moderate-relief interfluve areas, including the Mill Gulch site (Prentice et al., 2000, 2001), the Archae Camp site (Simpson et al., 1996), and the Murley site (Simpson et al., 1996). The Fort Ross Orchard site is in the interfluve area between the southern arm of Kollmer Gulch and Fort Ross Creek (Figure 3).

The linear shutter ridge that impounds alluvium at the Fort Ross Orchard site continues northwestward to Fort Ross Road, where another linear ridge continues nearly to Kollmer Gulch (Figure 3). Northwest of Fort Ross Road, a series of sag ponds demark a prominent fault strand along the southwestern side of this ridge. Brown and Wolfe (1972) show this fault as a dashed line and the primary fault as a solid line along the northeastern margin of the linear ridge (Figures 2 and 3), although the geomorphic expression of the western fault strand is greater in the area north of Fort Ross Road. We interpret that the Fort Ross Orchard site is at the southeastern end of a local left-step in the San Andreas Fault, which is in agreement with a similar interpretation made by C. Prentice (undated air-photo interpretation, personal communication, 2000). This interpretation differs from that made by Brown and Wolfe (1972), who mapped the primary fault strand along the northeastern side of the linear ridges and a secondary fault strand along southwestern side of the ridge (Figure 2).

As shown in more detail on Figure 4, the Fort Ross Orchard site includes a narrow, linear shutter ridge bordered on the northeast by the primary strand of the San Andreas Fault. The northeastern side of this ridge forms a 1- to 4-m-high fault scarp that faces uphill relative to the regional slope, and is associated with linear depressions that mark the location of the main strand of the San Andreas Fault (Figure 3). The linear ridge traversing the site acts as a buttress for alluvial-fan sediment derived from a small, incised drainage gulley northeast of the site (Figure 4). The trenches were excavated into alluvial-fan deposits derived from this gulley, which were laid down in the linear trough northeast of the linear ridge and across the primary fault strand

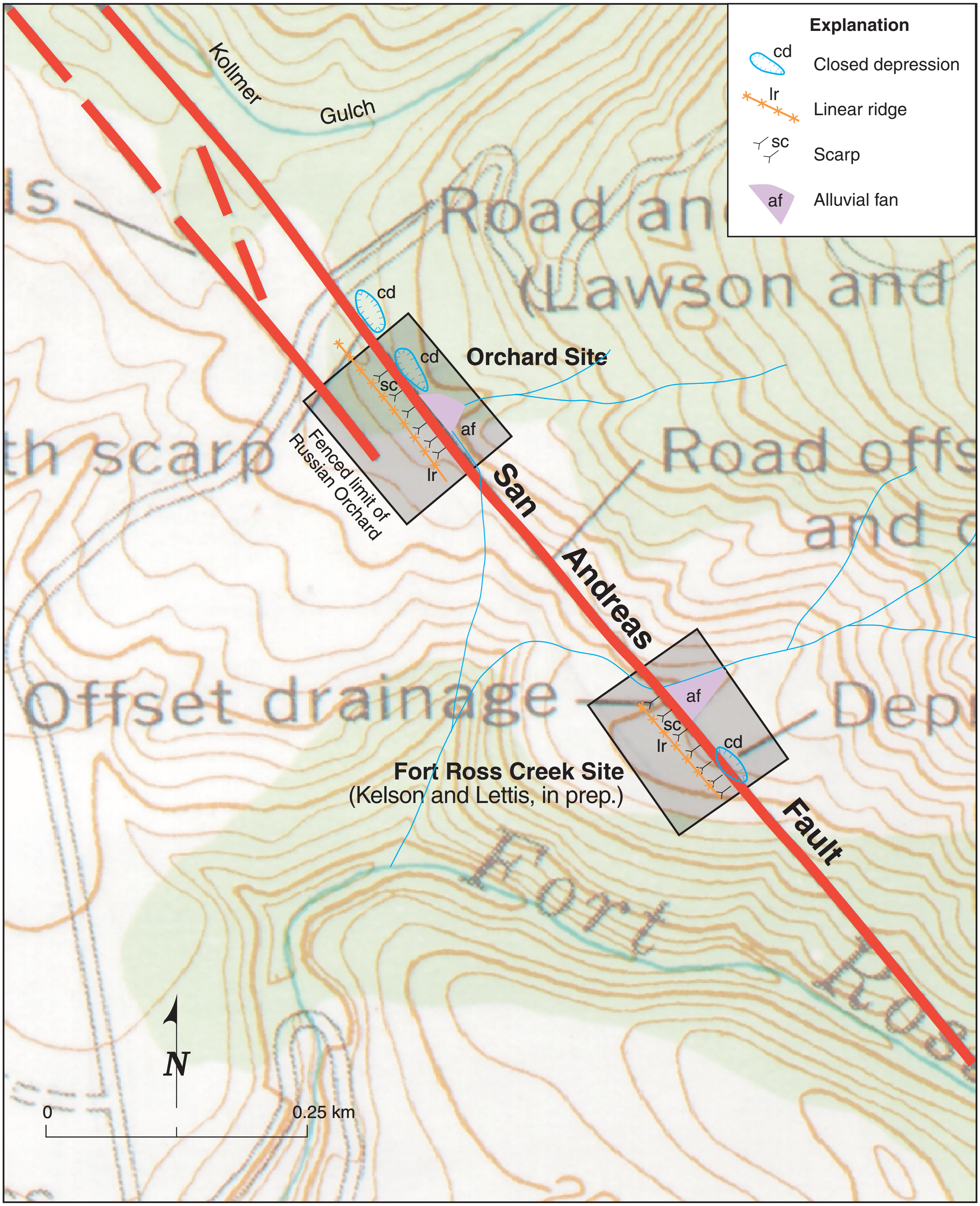

Figure 3. Enlarged fault map of Brown and Wolfe (1972), showing main strands of the San Andreas Fault and generalized geomorphic features at the Fort Ross Orchard site and the Fort Ross Creek site.

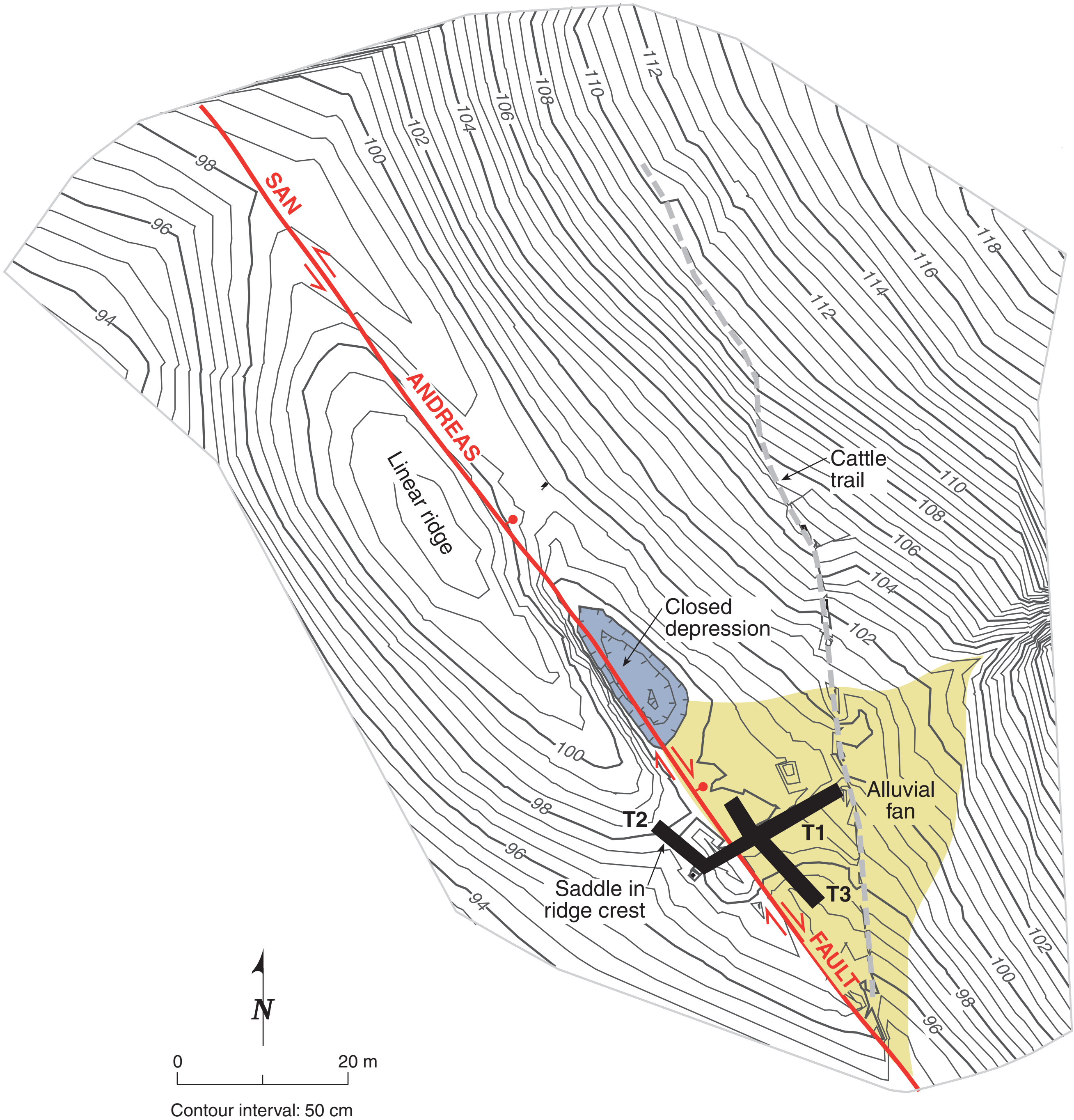

Figure 4. Detailed topographic map of the Fort Ross Orchard site showing San Andreas Fault and trenches T1, T2, and T3 (filled boxes).

(Figure 4). The alluvial fan forms the southeastern margin of the closed depression along the fault, which may be preserved as a geomorphic feature because of the fan deposition. Notably, the crest of the linear ridge is undulatory in the vicinity of the alluvial fan, where a 1-m-deep saddle is developed on the ridge crest (Figure 4). As discussed below, stratigraphic relations exposed in the trenches suggest that this saddle reflects a buried paleochannel that could be the southwestern extension of the present-day incised gulley northeast of the fault.

The Fort Ross Orchard site is of cultural significance because of the presence of several fruit trees planted by Russian colonists during their development and occupation of Fort Ross. This occupation began in early 1812, and the fort was completed and dedicated on August 12, 1812. The initial purpose of the fort was an outpost for hunting sea otter by the Russian-American Company, although by 1820 the otter population became so depleted that the colonists turned to agriculture and livestock, as a means to supply other Russian outposts in Alaska. Because of coastal fog, gophers, mice, and lack of sustained interest, the agricultural effort failed to produce enough goods to be economically viable. The small (approx. 50 x 150 m) orchard remaining near Fort Ross includes olive, pear, cherry, apple, and other fruit trees, although only a couple of the remaining trees are those that were originally planted by the Russian colonists. At present, there is no information indicating the presence of original orchard trees on the northeastern side of the fault, and there does not appear to be any linear arrangements of the trees that could be used as a piercing line to measure offset across the fault. The orchard is at an elevation of about 145 m (475 ft), which generally is just above the elevation of summer fog at Fort Ross. This elevation, coupled with the locally flat topography, probably was a main reason for locating the orchard at this site. In December 1841, the Russian-American Company sold the property to John Sutter (of Sutter's Fort near Sacramento), and Fort Ross was abandoned within a few months. The orchard does not appear to have been maintained after abandonment by the Russian colonists, although there is evidence that later ranching operations included construction of a fence line through the site (D. Murley and B. Walton, Fort Ross State Historic Park rangers, personal communication, 2001). Based on this site history, the orchard likely was not being maintained during the 1906 surface rupture, and the site has not undergone substantial cultural modification.

3.0
PALEOSEISMIC RESULTS

This research at the Fort Ross Orchard site was aimed at characterizing the timing of late Holocene paleoearthquakes and estimating a geologic slip rate on the northern San Andreas Fault. The focus of our effort was to identify geologic evidence of past large earthquakes and develop preliminary age estimates for the ruptures. The scope of work included generating a detailed topographic map of the Orchard site, and excavation of one trench across the fault and through late Holocene alluvium within the depositional basin, as well as two fault-parallel trenches (one on each side of the fault) at the site. This exploratory paleoseismologic research, which was conducted in November and December 2000, is the first documentation of shallow geologic conditions across the San Andreas Fault at this site.

Our efforts at the Fort Ross Orchard site were designed to expose faulted and unfaulted stratigraphy across the 1906 rupture of the San Andreas fault, and to evaluate possible evidence of pre-1906 ruptures. To this end, we excavated trench 1 (Figure 4) across the east-facing fault scarp and into the linear depression. In addition, we excavated two fault-parallel trenches (trenches 2 and 3, Figure 4) to investigate the possibility of a late Holocene paleochannel that might be a piercing line for evaluating fault slip rate. Based on these efforts, the site yielded limited information on the timing of past earthquakes but did not yield robust data on fault slip rate.

3.1 Trench Stratigraphy

The three trenches at the Fort Ross Orchard site exposed a fairly straight-forward sequence of late Holocene and historic deposits overlying weathered sandstone bedrock (Figures 5, 6, and 7). In general, the bedrock northeast of the fault scarp is overlain by two massively bedded alluvial-fan deposits, two discontinuous swale-fill deposits, and a series of post-1906 alluvial and colluvial deposits. For ease of description, we herein refer to these surficial deposits as the Lower, Middle and Upper Alluviums, respectively (units ❷ through ❾, Figures 5, 6, and 7). Information on the three-dimensional geometry of these deposits is available at the site because of the orientations of trenches 1 and 3 (Figure 4). Surficial deposits at the site also include discontinuous colluvial or fissure-fill deposits locally adjacent to the San Andreas fault that may be directly related to earthquake rupture. In addition, trench 2 exposed a paleochannel incised into the sandstone bedrock that is filled with a mixture of alluvium and colluvium (units C1 and C2, Figure 6). The lithologic characteristics of these deposits are summarized in the following text, and are provided in more detail on Figure 5b.

Trenches 1 and 2 exposed bedrock southwest of the San Andreas fault (unit ❶, Figures 5 and 7), consisting of sheared sandstone within the Paleocene German Rancho Formation (Wagner and Bortugno, 1982). In the northeastern part of the site, trench 1 exposed extremely weathered clay with gravel that appears to be weathered Paleocene or Cretaceous bedrock. The stratigraphically oldest surficial deposit overlying these bedrock units is the Lower Alluvium, which consists of two massively bedded alluvial-fan deposits (units ❷ and ❸; Figures 5 and 7). Both of these units are generally uniform throughout the site, consisting of a nearly saturated silty clay (unit ❷) at

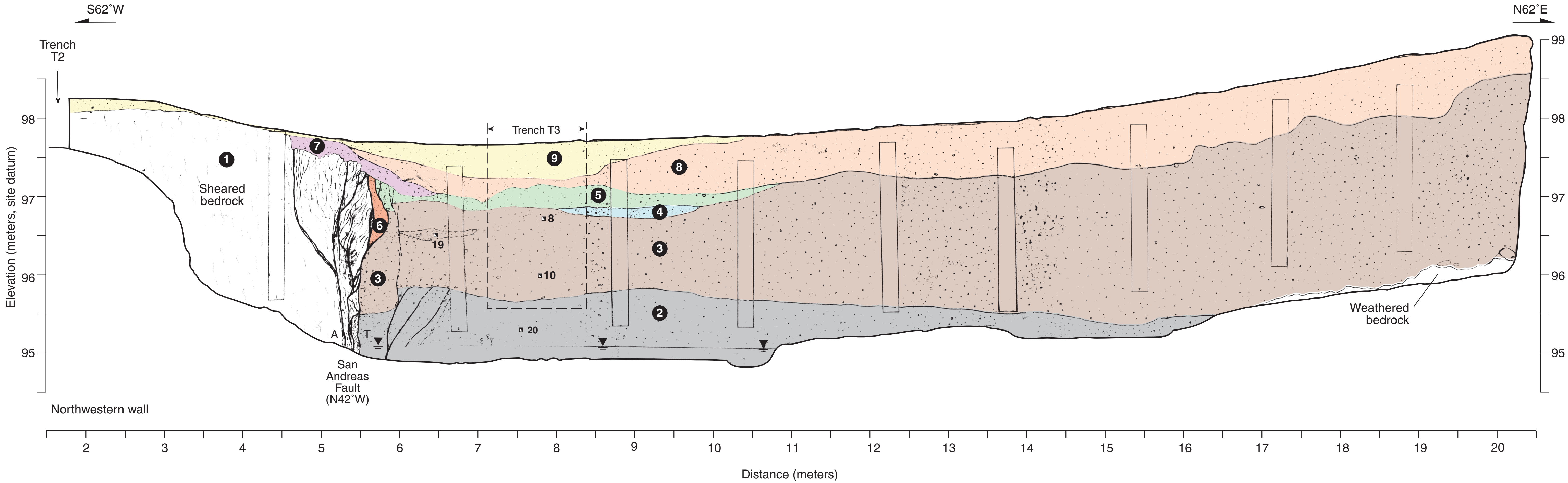

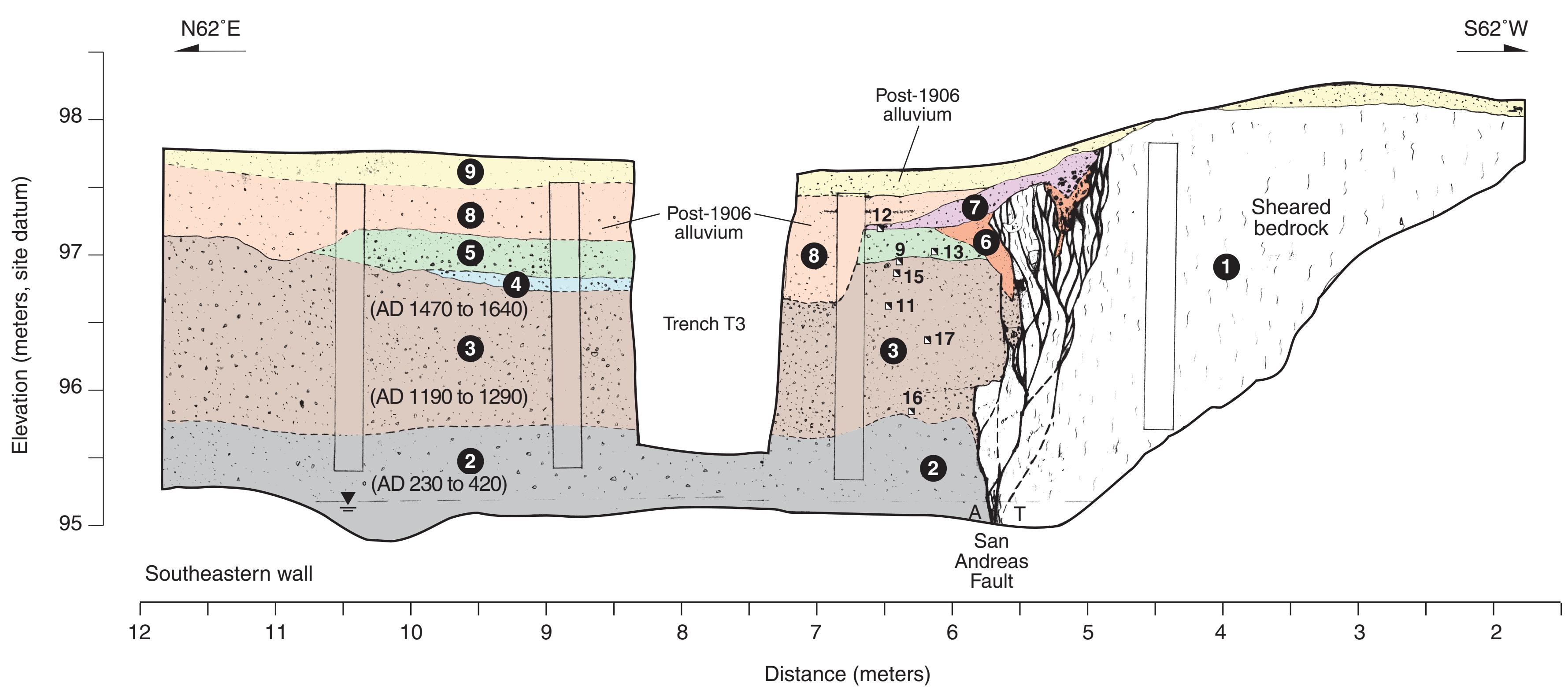

Explanation

8 Radiocarbon sample (see Table 1)

(K) Krotovina (filled burrow or root cast)

Note: For Unit descriptions, see Figure 5b.

ORCHARD SITE
FORT ROSS STATE HISTORIC PARK

Log of Trench 1
North and South Walls

WLA William Lettis & Associates

Figure 5a

1377 Ft. Ross

Unit 9 : Historic alluvium and colluvium (associated with present-day ground surface). *On crest of linear ridge, southwest of fault*: Brown (7.5YR 4/4) SILTY SAND (SM); fine to medium sand; 10% gravel near base, grading to 5% gravel near top; subangular gravel up to 10 mm composed of yellow weathered sandstone; moderately sorted; medium dense; dry; clear irregular basal contact. *Along fault and in depositional basin northeast of fault*: Very dark grayish brown (10YR 3/2) SILTY SAND (SM); fine to medium sand; 5% gravel; subangular gravel up to 5 mm composed of red and orange weathered sandstone; moderately sorted; moist; loose; slightly sticky, slightly plastic; gradual smooth basal contact. *In southeastern part of trench 3*: Very dark grayish brown (10YR 3/2) GRAVELLY SAND (SW); fine to medium sand; 5 to 15% gravel; angular to subangular gravel up to 30 mm composed of red and orange weathered sandstone; crude bedding; moderately sorted; loose; moist; non-sticky, non-plastic; grades into silty sand to northwest along fault; contains barbed wire and pieces of sawn redwood; clear irregular basal contact; represents present-day outlet swale from depositional basin northeast of fault (UPPER ALLUVIUM).

Unit 8 : Historic alluvium. Very dark brown (10YR 2/2) SILTY SAND (SM); fine to coarse sand; 5 to 15% gravel; subangular to subrounded gravel up to 15 mm composed of orange and red weathered sandstone; moderately sorted; loose to medium dense; moist; sticky, slightly plastic; locally contains charcoal fragments and pieces of sawn redwood; gradual irregular basal contact; irregular contact probably a result of local cultural modification; deposit primarily derived from sheetwash and alluvial-fan deposition from northeast (UPPER ALLUVIUM).

Unit 7 : Historic colluvium. Very dark grayish brown (10YR 3/2) CLAYEY SILT WITH GRAVEL (ML); located only adjacent to fault zone; fines eastward; southwestern half contains gravel up to 20 mm; northeastern half contains gravel up to 10 mm; gravel clasts are angular red and orange weathered sandstone; poorly sorted; moist; medium stiff; not sheared and not faulted; clear smooth basal contact; derived from tectonic fault scarp (SCARP-DERIVED COLLUVIUM).

Unit 6 : Historic colluvium / alluvium / fissure filling. Very dark grayish brown (10YR 3/2) to very dark brown (10YR 2/2) CLAYEY SAND WITH GRAVEL (SW) to SILTY SAND (SM); located only adjacent to fault zone; triangular shaped body within fault zone (Trench 1, SE wall, station 5.5 m) contains gravel up to 25 mm, composed of clasts of friable weathered sandstone (unit), clasts have crude subvertical alignments, unit contains possible shear fabric; tabular-shaped bodies adjacent to fault zone (Trench 1, SE wall, station 6 m and NW wall, station 5.5 m) contain fine to medium sand, 5% gravel clasts up to 7 mm composed of weathered sandstone, these silty sand bodies contain possible internal shear fabric and are faulted; overlain unconformably by unit ; possible fissure-fill deposit or sheared colluvium/alluvium.

Unit 5 : Late Holocene alluvium. Very dark grayish brown (10YR 3/2) GRAVELLY SAND (SW); fine to coarse sand; 25 to 35% gravel; subangular to subrounded clasts up to 25 mm composed of orange and red weathered sandstone; poorly sorted; medium dense to dense; moist; contains rare charcoal fragments; faulted; clear smooth basal contact; deposit primarily derived from sheetwash and alluvial-fan deposition from northeast (MIDDLE ALLUVIUM).

Unit 4 : Late Holocene alluvium. Very dark gray (10YR 3/1) SILTY SAND WITH GRAVEL (SM); fine to coarse sand; 20 to 25% gravel; subrounded to subangular clasts composed of orange and red weathered sandstone; medium dense; moist; contains rare charcoal fragments; abrupt smooth basal contact; deposit is narrow tabular body of relatively constant thickness (about 10 cm), oriented parallel to fault and dipping northwest toward closed depression; alluvial swale deposit (MIDDLE ALLUVIUM).

Unit 3 : Late Holocene alluvium. Very dark brown (10YR 2/2) SILTY SAND WITH GRAVEL (SM); fine to coarse sand; 20 to 30% gravel; subangular to subrounded clasts up to 40 mm composed of orange and red weathered sandstone; poorly sorted; massive; moist; medium dense; faulted; contains common charcoal fragments; in Trench T1 (NW wall, station 6 to 7 m) includes strong brown (5YR 4/6) SILT (ML), discontinuous bed with abundant charcoal fragments up to 15 mm long (possible *in-situ* burn layer); gradual smooth basal contact; alluvial-fan deposit (LOWER ALLUVIUM).

Unit 2 : Late Holocene alluvium. Very dark gray (10YR 3/1) SANDY CLAY (CL); fine to coarse sand; 10 to 20% gravel; subangular to subrounded clasts composed of red and orange weathered sandstone; massive; moist to wet; contains seeps in trench wall near fault; sticky, plastic; contains rare charcoal fragments; faulted; basal contact not observed; alluvial-fan deposit (LOWER ALLUVIUM).

Unit 1 : Weathered bedrock. *Beneath linear ridge, southwest of fault*: Reddish yellow (7.5YR 6/8) to yellow (2.5Y 7/6) SHEARED SANDSTONE; fragments of coherent sandstone up to 15 mm; otherwise pervasively sheared; dry. *Within fault zone*: Strong brown (7.5YR 4/6) CLAY (CL), pervasively sheared; fragments of coherent sandstone up to 10 mm; sticky, plastic; moist. *In northeastern part of Trench 1*: Red (2.5YR 4/8) and yellowish red (5YR 5/8) CLAY WITH GRAVEL (CL); heterogeneous mixture of clay and gravel clasts, with sandstone clasts up to 20 mm (GERMAN RANCHO FM.).

Unit C2: Late Holocene colluvium: Very dark brown (10YR 2/2) CLAYEY SILT WITH GRAVEL (ML); 10 to 20% gravel; angular to subrounded clasts up to 10 mm composed of yellow sandstone; poorly sorted; massive; dry; stiff; clear smooth basal contact; colluvial swale-fill deposit.

Unit C1: Late Holocene alluvium / colluvium: Very dark grayish brown (10YR 3/2) GRAVEL WITH CLAY (GW); 50 to 70% gravel; angular to subangular clasts up to 60 mm composed of yellow sandstone, and rare subrounded clasts up to 10 mm composed of red sandstone; one rare subrounded sandstone clast 250 mm in diameter; dense; abrupt irregular basal contact cut into bedrock; colluvial swale-fill deposit or alluvium.

Figure 5b. Lithologic descriptions of units in trenches 1, 2, and 3, Fort Ross Orchard site.

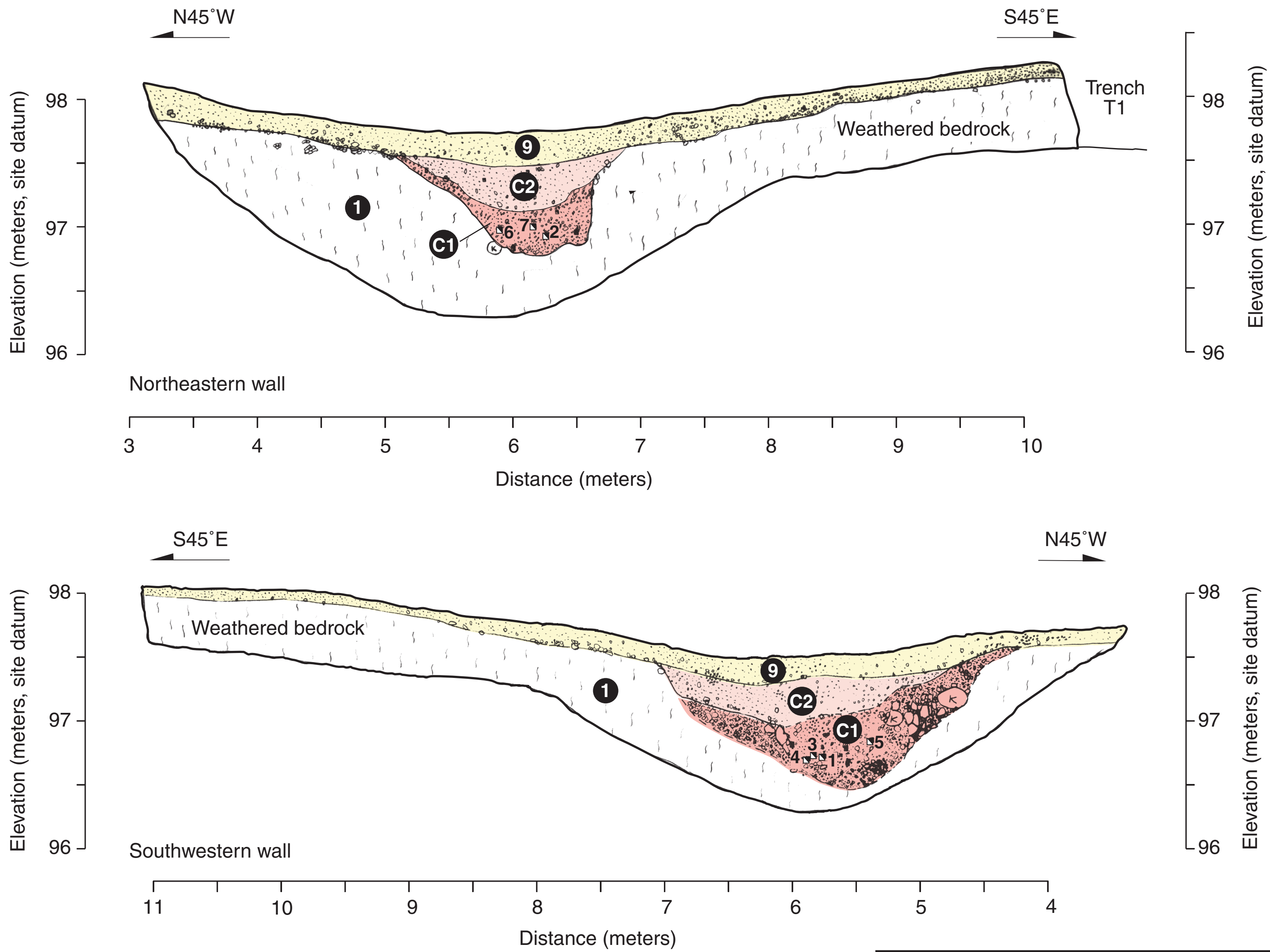

Explanation

2 ◪ Radiocarbon sample (see Table 1)

Note: For unit descriptions, see Figure 5b.

ORCHARD SITE
FORT ROSS STATE HISTORIC PARK

Log of Trench 2

WLA William Lettis & Associates

Figure 6

1377 Ft. Ross

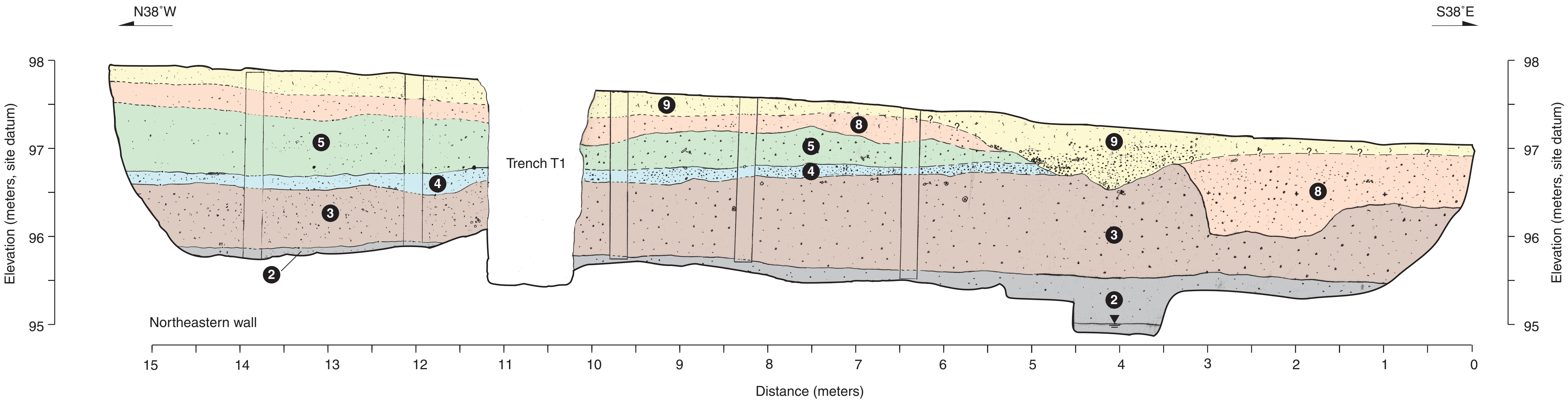

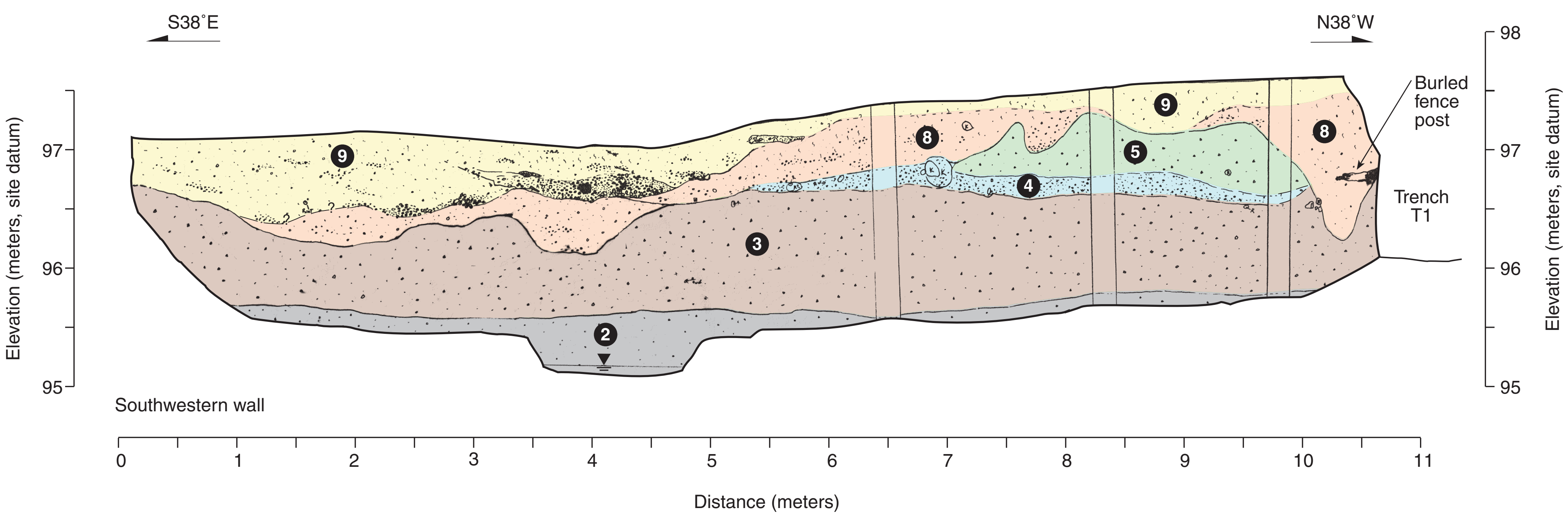

Note: For unit descriptions, see Figure 5b.

ORCHARD SITE FORT ROSS STATE HISTORIC PARK	
Log of Trench 3	
WLA William Lettis & Associates	Figure 7

1377 Ft. Ross

the base of the trenches and a poorly sorted silty sand with gravel (unit ❸). Based on the presence of bedrock in the northeastern part of trench 1 (Figure 5), unit ❷ appears to have been deposited in a linear basin adjacent to the San Andreas Fault at the site. The three-dimensional exposure of unit ❸ provided by trenches 1 and 3 shows that this deposit is thickest near the apex of the alluvial fan (Figure 4), and thins both to the southwest in trench 1 (Figure 5) and to the northwest in trench 3 (Figure 7). Thus, we interpret that the bulk of the alluvial fan derived from the northeastern gulley at the Fort Ross Orchard site is composed of sediments that are part of, or are similar to, unit ❸. These relations suggest that the linear shutter ridge at the Fort Ross Orchard site had at least an incipient ancestor during the time of unit ❸ deposition. As summarized below, multiple radiometric age determinations from unit ❸ suggest that this alluvial-fan sedimentation occurred over a period of at least several hundred years.

Locally overlying unit ❸ is the Middle Alluvium, which includes units ❹ and ❺ (Figure 5 and 7). Unit ❹ is a distinct, laterally discontinuous silty sand with gravel that reflects a change in the type of sedimentation northeast of the fault at the site. Based on the exposures in trenches 1 and 3, this deposit is a thin (10 cm) sand bed oriented parallel with the fault trace. It is only about 2 m wide, but more than 10 m long, extending throughout most of the northeastern wall of trench 3 (Figure 7). The deposit dips gently to the northwest, and is interpreted to represent a small, linear swale that transmitted water and sediment from the alluvial-fan apex northwestward into the closed depression at the site (Figure 4). Later erosion affiliated with units ❽ and ❾ (Figure 7) appears to have removed the southeastern part of this deposit, as noted below. Similarly, unit ❺ has a comparable orientation, but is slightly wider and thicker (see northwestern wall of trench 1, Figure 5). We interpret that the Middle Alluvium (units ❹ and ❺) reflects deposition on the northwestern part of the alluvial fan at the site.

Stratigraphically between the Middle and Upper Alluviums at the Fort Ross Orchard site are units ❻ and ❼, both of which are only within or directly adjacent to the fault zone, and appear to be intimately related to surface rupture along the fault (Figure 5). Unit ❻ consists of three separate bodies of sediment exposed in trench 1, a triangular shaped body within the fault zone exposed on the SE wall (station 5.5 m), and two tabular bodies on the northeastern margin of the fault zone (SE wall, station 6 m and NW wall, station 5.5 m; Figure 5). The triangular body at station 5.5 m on the SE wall of trench 1 contains clasts of friable sandstone with subvertical orientations, within a clayey sand matrix that has some evidence of shear fabric. The sandstone clasts in the deposit were derived from the adjacent sheared sandstone bedrock. This body lies within the fault zone, although the margin of the deposit, if sheared, is comparatively less deformed than the surrounded bedrock. Unit ❻ is interpreted as either a deposit that fills a rupture-related fissure, or a sliver of surficial colluvium or alluvium caught up within the fault zone. The other two bodies included within unit ❻ are composed primarily of silty sand that is sheared and faulted by individual strands of the fault zone. These bodies may be tectonically detached slivers of alluvium deformed by fault movement, or deformed slivers of older fissure fills.

Unit ❼ is unique among deposits at the Fort Ross Orchard site, because it clearly is a colluvium derived from erosion of the San Andreas Fault scarp (Figure 5). This deposit overlies the majority of the fault zone, and consists of a poorly sorted mixture of silt, gravel, sand, and clay. The colluvium is finer toward the east, and gravel clasts within the deposit are smaller and less abundant to the east, away from the fault (Figure 5). Unit ❼ is not faulted, and thus represents colluvial deposition following the most-recent surface rupture at the site.

The Upper Alluvium at the Fort Ross Orchard site contains two deposits that overlie unit ❼ and thus post-date the most-recent surface rupture at the site (units ❽ and ❾, Figures 5 and 7). Both of these deposits are alluvial sands, with various amounts of silt, gravel, and clay. Unit ❽ is nearly a meter thick at the northeastern end of trench 1 and thins where it onlaps onto the fault scarp, suggesting that it was derived from the northeast through alluvial-fan and sheetwash processes. At the far southeastern end of the site (see SE end of trench 3; Figure 7), an abrupt erosional contact at the base of unit ❽ suggests that channelized flow draining the site may have returned to a southeasterly flow direction. Locally, the deposit includes cultural artifacts, including barbed wire and sawn or milled pieces of redwood that appear to be fence posts. This deposit may be a result of land-use changes (i.e., forest harvesting) in the local watershed during the early 20^{th} century, and associated increases in sediment production and deposition. The highly irregular basal contact of unit ❽ at the intersection of trenches 1 and 3 (Figure 7, station 10 m) suggests that cultural excavations related to fence building extended at least 1 m deep locally along the base of the fault scarp. Lastly, unit ❾ represents the deposits directly beneath the ground surface, and includes three facies (Figures 5, 6, and 7): poorly sorted silty sand that is the active scarp-derived colluvium from the linear ridge, moderately sorted silty sand within the present-day depositional basin northeast of the fault, and coarser gravelly sand associated with the present-day swale outlet from the basin. All three of these facies are gradational. Overall, unit ❾ thickens to the southeast toward the present-day outlet of the linear depression. The sandy alluvium in the present-day swale outlet crosses trench 3 at its southeastern end, trends along the fault trace through the site, and ultimately flows to Fort Ross Creek (Figure 3).

Trench 2 exposed a distinct paleochannel beneath a topographic saddle in the crest of the linear shutter ridge, across which we excavated to investigate the possibility of obtaining a piercing line across the San Andreas Fault (Figure 4). The paleochannel is about 2 m wide and is incised abruptly into the sandstone bedrock. The channel thalweg plunges steeply (about 16˚) to the southwest. Within this paleochannel are two deposits (units C1 and C2; Figure 6) that reflect the remnants of channel alluvium mixed with swale-filling colluvium. The lower deposit (unit C1, Figure 6) is much coarser than any other surficial deposit exposed at the site, containing clasts as large as 250 mm. Several of the sandstone clasts within this paleochannel are subrounded and imbricated, suggesting deposition by channelized flow. The arrangement, size, and rounding of these clasts are unique in the exposures at the site, and suggest that the small gulley northeast of the fault previously flowed across the shutter ridge. Unit C2 overlies unit C1 within the bedrock notch, but is considerably finer grained, and does not contain large rounded sandstone clasts. This poorly sorted deposit is interpreted as colluvium that filled the topographic swale above the incised channel after its abandonment. Similarly, the present-day hillslope colluvium (unit ❾; Figure 6) thickens slightly above the paleochannel, and represents continued smoothing of the ridge-crest topography through time.

3.1.1 Age Estimates

The age estimates for the surficial deposits at the Fort Ross Orchard site are based on the presence of historic cultural items and radiometric analyses of charcoal fragments. Charcoal fragments were fairly abundant within some of the stratigraphic units, but were not present in many of the units. A total of 57 samples were collected from various stratigraphic units exposed in trenches 1, 2, and 3. We sampled only angular charcoal fragments that appeared to have not been reworked or altered. Of the 57 charcoal fragments, 18 samples were analyzed for radiocarbon age determination by the Center for Accelerator Mass Spectrometry (CAMS) at Lawrence Livermore Laboratories (Table 1), under the guidance of G. Seitz and J. Southon. The stratigraphic position of these charcoal fragments and their importance to estimating the ages of deposits at the Fort Ross Orchard site are described below.

One charcoal sample was analyzed from the lowermost surficial stratum exposed in the trenches (unit ❷, Figure 5; sample FR-20, Table 1). This sample yielded a calibrated age of AD 230 to 420, which seems reasonable for this deposit given its stratigraphic position and the site geomorphology. The overlying massive alluvial deposit (unit ❸) yielded multiple charcoal fragments, eight of which were analyzed. These eight samples can be divided into two populations, including those in the upper or lower parts of this unit. The lower part of the alluvium contains two samples (samples FR-10 and FR-16; Table 1), both of which yielded ages older than about AD 1300. However, these two samples are stratigraphically inconsistent, with the sample from the very basal part of unit ❸ (FR-16, Figure 5) providing an age-date younger than sample FR-10, which was about 30 cm higher. Assuming that one of these samples correctly estimates the age of the deposit, then either one is re-worked older charcoal, or one has been introduced into the sediments after deposition (i.e., through burrowing animals or another biologic process). Because re-working older charcoal is more likely at this site than burrowing (there is no evidence for burrowing near these samples), the younger age-date is more likely to be the correct date. Thus, we consider the lower part of unit ❸ to be about AD 1190 to 1290 in age.

The six samples from the upper part of unit ❸ generally range in age from AD 1440 to 1660 (Table 1). The exception is sample FR-11, which was taken from the same stratigraphic position but clearly is an outlier from this sample population. Thus, we believe that sample FR-11 is a re-worked piece of charcoal that does not reflect the age of the deposit. Given this, the average age of the population of five samples from the upper part of unit ❸ is AD 1470 to 1640. The age-dates from unit ❸ samples are all younger than the single age-date obtained from the overlying deposit (sample FR-13, unit ❺, Table 1). Because of this inconsistency of age with stratigraphic position, we interpret also that sample FR-13 is not representative of the age of unit ❺.

Lastly, we analyzed one sample from the scarp-derived colluvium exposed in trench 1 (sample FR-12, unit ❼, Table 1). This sample yielded an age of AD 1640 to present, which is consistent with deposition during historic time. As noted above, the unit directly above unit ❼ (unit ❽, Figures 5 and 7) contains historical cultural items, including barbed wire and remnants of redwood fence posts. Given these relations, we interpret that the scarp-derived colluvium (unit ❼, Figure 5) was most likely deposited following the 1906 surface rupture at the site. Units ❽ and ❾ have been deposited since this earthquake, and represent historic accumulations of sediments within the linear depression northeast of the shutter ridge at the Fort Ross Orchard site.

Trench 2 exposed a paleochannel cut into the sandstone bedrock, and we analyzed seven charcoal samples taken from the alluvium filling this paleochannel (unit C1, Table 1). These

Table 1 Summary of Radiocarbon Ages, Fort Ross Orchard Site

Sample No.	Lab No.[@]	Conventional ^{14}C Age (yr BP ± 1σ)	Calibrated Age (cal. yr AD)[#] (2σ, 95% probability)	Interpreted Age-estimate[%]
TRENCH 1				
Unit 7 Scarp-derived Colluvium				***AD 1906***
FR-12	71277	200 ± 40	AD 1640 to present	
Unit 5 Alluvium				
FR-13	71524	800 ± 40	(AD 1160 to 1280)	
Upper Unit 3 Alluvium				***AD 1470 to 1640***
FR-9	71274	330 ± 40	AD 1450 to 1650	
FR-15	71525	310 ± 40	AD 1470 to 1660	
FR-8	71273	360 ± 50	AD 1440 to 1650	
FR-11	71276	650 ± 40	(AD 1280 to 1400)	
FR-19	71528	320 ± 40	AD 1460 to 1660	
FR-17	71527	370 ± 40	AD 1440 to 1640	
	Average:		*AD 1470 to 1640*	
Lower Unit 3 Alluvium				***AD 1190 to 1290***
FR-10	71275	1130 ± 40	(AD 780 to 1000)	
FR-16	71526	770 ± 40	AD 1190 to 1290	
Unit 2 Alluvium				***AD 230 to 420***
FR-20	71614	1730 ± 40	AD 230 to 420	
TRENCH 2				
Unit C1 Alluvium				***AD 1260 to 1390***
FR-5	71272	1140 ± 50	(AD 780 to 1020)	
FR-7	71523	700 ± 40	AD 1260 to 1390	
FR-3	71270	3230 ± 50	(1680 to 1410 BC)	
FR-6	71522	810 ± 40	(AD 1160 to 1280)	
FR-1	71521	980 ± 40	(AD 990 to 1160)	
FR-4	71271	1540 ± 50	(AD 410 to 640)	
FR-2	71269	1150 ± 40	(AD 780 to 980)	

Samples are listed in stratigraphic order, with stratigraphically highest samples at the top.
@ All samples analyzed by CAMS, Livermore, California
\# Calibrated based on Stuiver and Reimer (1993), using CALIB v4.3 (2000). Averages are equally weighted. Parentheses indicate stratigraphically inconsistent samples (not included in average).
% Interpreted based on 2-sigma ranges in sample averages, rounded to decade.

samples yielded an extremely wide range in age-dates (from 1680 BC to AD 1390), with no distinct groupings or populations of age-dates. Because this deposit represents an alluvial channel fill, many (if not all) of the samples probably were pieces of re-worked charcoal. We interpret that the youngest age-date of the seven samples is the closest representation of the true age of the deposit (sample FR-7, Table 1). This sample was taken from the center of the unit C1 deposit on the northeastern wall of trench 3 (Figure 6), and provided an age-date of AD 1260 to 1390. Thus, we interpret that the age of unit C1 is AD 1260 to 1390, which is comparable in age to unit 3 exposed in trenches 1 and 3.

3.1.2 Stratigraphic Interpretation

The three-dimensional trench exposures at the Fort Ross Orchard site provide an opportunity to assess the distribution of sediments and processes of deposition. As noted above, alluvial-fan sediments derived from the small gulley directly northeast of the site dominate the stratigraphic record. These sediments are preserved primarily because of uplift along the fault and formation of the linear shutter ridge, which has acted, over the past several hundred years, as a sediment dam. In general, the sediments derived from the gulley have begun filling up the linear trough that lies directly northeast of the fault, although the presence of the closed depression northwest of the trenches (Figure 4) shows that the filling is local and incomplete. The lowermost alluvial deposits (units ❷ and ❸, Figures 5 and 7) are massive sandy clay and silty sand deposits that represent fine-grained alluvial-fan deposition. Available age estimates suggest that there may have been a substantial depositional hiatus or period of erosion between units ❷ and ❸, because these units are estimated to be about 770 to 1,060 years different in age (Table 1). The age-dates suggest that unit ❸ was deposited over a time period of about 200 to 450 years, and the massive nature of this deposit suggests that it was probably laid down slowly and consistently over this time period. The three-dimensional exposures show that units ❹ and ❺ filled a small swale that probably trended southwesterly toward the fault, encountered the shutter ridge, and then trended northwesterly parallel to the fault and into the closed depression. This represents a flow direction that is opposite to the present-day slope of the linear trough in the southwestern part of the site (Figure 4).

The discontinuous nature of unit ❻ makes interpretation of its origin difficult, although its preservation primarily along the San Andreas Fault suggests that it is related to fault displacement. As described above, unit ❻ consists of three separate bodies of sediment within the fault zone, including a triangular body on the SE wall of trench 1 that contains clasts of friable sandstone with subvertical orientations. Unit ❻ is interpreted as either a deposit that fills a rupture-related fissure, or a sliver of surficial colluvium caught up within the fault zone. The other two bodies included within unit ❻ are composed primarily of silty sand that is sheared and faulted by individual strands of the fault zone. These bodies may be tectonically detached slivers of alluvium deformed by fault movement, or deformed slivers of older fissure fills. Because these sediments are sheared, they pre-date the 1906 rupture, and some or all of the shearing probably may have been caused by the 1906 faulting. If the sediments are sheared material that filled a pre-1906 fissure, unit ❻ may be evidence of an earlier surface rupture at the Fort Ross Orchard site. However, because of an absence of clear evidence of an earlier surface rupture is not present from these exposures, we cannot provide well-founded data of such an event. Additional exposures at the Fort Ross Orchard site and additional age-dating of charcoal samples from unit ❻ may provide better information on the occurrence and timing of this possible pre-1906 surface rupture.

Colluvial unit ❼ was derived from erosion of the San Andreas Fault scarp (Figure 5). The lithology and angularity of the gravel clasts are similar to the sandstone bedrock that comprises the northeast-facing fault scarp. The colluvium is finer toward the east, and gravel clasts within the deposit are smaller and less abundant to the east, away from the fault (Figure 5). Unit ❼ is not faulted, and thus represents colluvial deposition following the most-recent surface rupture at the site. In addition, unit ❼ is directly overlain by unit ❽, which contains abundant historical items and was deposited within the past hundred years. Thus, unit ❼ represents colluviation from the San Andreas Fault scarp following the 1906 rupture. Units ❽ and ❾ reflect deposition within the linear trough northeast of the fault since the 1906 rupture, with unit ❽ forming as a combination of southwestward alluviation from the small gulley and cultural deposition. This unit has been disturbed locally within the past hundred years, probably as a result of construction of a fence line through the site (D. Murley and B. Walton, Fort Ross State Historic Park, personal communication, 2001). Unit ❾ contains several facies that collectively represent the active depositional processes at the Fort Ross Orchard site, including active colluviation on the shutter ridge, alluvial-fan deposition in the linear trough, and alluvial channel deposition in the swale draining southeasterly from the linear trough (Figure 4).

Because of erosion of older deposits by units ❽ and ❾ in the southeastern part of the site (Figure 7), it seems unlikely that deposits more than a hundred years or so would be preserved along the fault to the southeast of trench 3 (Figure 4). Thus, we postulate that additional paleoseismic investigations in the southeastern part of the Fort Ross Orchard site likely would not yield information on the timing of pre-1906 ruptures on the San Andreas Fault. However, preservation of pre-1906 deposits along the fault is likely in the area northwest of trench 1 and near the closed depression (Figure 4), because the young alluvial fan has essentially protected this area from degradation.

3.2 Trench Geologic Structure

The primary strand of the San Andreas Fault is exposed in trench 1, where it deforms sandstone bedrock and the surficial deposits older than unit ❼ (Figure 5). In general, the fault zone is narrow (less than 1 m wide), and has a cross-trench strike of N42˚W. We observed no reliable indicators of slip direction in the trench exposures (e.g., slickensides, drag features), although it can be assumed based on historical observations (Lawson, 1908) and site geomorphology that the fault is dominated by right-lateral offset with a component of southwest-up vertical separation. The main fault zone exposed in trench 1 is only about 50 to 60 cm wide at the bottom of the trench, but it broadens to a width of about 1 m near the ground surface (Figure 5). The zone contains multiple anastomosing strands primarily within the sheared bedrock, although some strands border lentil-shaped bodies of sediments (including parts of units ❸ and ❻; Figure 5). The rock masses between primary fault strands generally are pervasively sheared; shearing within the surficial sediments is considerably less developed. Bedrock on the southwestern side of the fault is sheared and deformed over a distance of at least 2 m from the main fault zone exposed in the trench. The bedrock is progressively less sheared in a southwesterly direction from the fault, although even away from the fault zone the bedrock is weathered and friable

(Figure 6). As noted above, none of the fault strands exposed in trench 1 extends into unit ❼ or overlying surficial deposits.

Most of the fault strands extend upward to the base of unit ❼, although a few notable strands extend upward only to distinct lower stratigraphic contacts (Figure 5). For example, on the northwestern wall of trench 1, three southwesterly dipping fault strands deform unit ❷ but are truncated by unit ❸ (station 6.5 m, NW wall, Figure 5). Of these three strands, the southwestern strand has a branch that extends into overlying units and to the base of unit ❼. On the southeastern wall of the same trench, there are no strands that are truncated by unit ❸; instead there is only a single strand that extends upward and forms the contact between unit ❸ and bedrock (station 6 m, SE wall, Figure 5). We could not follow this strand upward above the location of bedrock, where it would be entirely within the massive alluvium of unit ❸. Thus, upward fault terminations exist within the lower alluvium on both walls of the trench, although these terminations occur at different stratigraphic levels. In a previous report (Kelson and Lettis, 2001), we postulated that these trench relations suggest the possibility of as many as three pre-1906 earthquakes. Unfortunately, there are no other corroborating lines of evidence for these possible paleo-earthquakes at this site.

INTERPRETATION AND DISCUSSION

The primary goal of this investigation of the northern San Andreas Fault at the Fort Ross Orchard site is to provide information on the late Holocene paleoseismic history of surface-rupture earthquakes. The history of past earthquakes on the North Coast segment includes the occurrence of at least five surface-rupturing earthquakes during the past 2000 years near Point Arena (Prentice, 1989), and the occurrence of at least seven surface ruptures within the past 2,000 to 2,500 years at Vedanta (Figure 1; Niemi et al., 2002). Knudsen et al. (2001) interpret geologic evidence to indicate the occurrence of three events (including the 1906 earthquake) within the past thousand years or so at Bolinas Lagoon (Figure 1). Collectively, these studies indicate a range in recurrence for large earthquakes on the North Coast segment of the San Andreas Fault of 180 to 370 years (WGCEP, 2003). Our investigation at the Fort Ross Orchard site provides supplementary information to help confirm and refine the existing body of knowledge.

Results from the Fort Ross Orchard site confirm the previously well-established occurrence of surface rupture along the San Andreas Fault near this site during the 1906 rupture (Lawson, 1908; Prentice, 1989; Noller and Lightfoot, 1997). The presence of an unfaulted scarp-derived colluvium at the site (unit ❼, Figure 5) is consistent with the site geomorphology and reports of local uplift and scarp production during the 1906 rupture (Lawson, 1908). Radiometric data from this unit are consistent with a modern age-estimate and stratigraphic position relative to deposits containing historical items. Thus, we interpret that closely following the 1906 rupture at the Fort Ross Orchard site, partial erosion of the northeast-facing fault scarp resulted in deposition of colluvium (unit ❼), and that this deposit has since been overlain by more recent alluvial-fan and colluvial deposits.

In addition, we interpret the possibility of up to three pre-1906 earthquakes on the North Coast segment of the San Andreas Fault at the Fort Ross Orchard site. However, available stratigraphic and radiometric data not provide strong constraints on the occurrence and timing of these pre-1906 earthquakes. The trench exposures provide equivocal evidence, in the form of limited upward fault terminations, which could provide information on the timing of past surface ruptures. For example, if the upward fault termination at the base of unit ❸ exposed on the northwestern wall of trench 1 (station 6.5 m, Figure 5) reflects a past rupture, this rupture occurred between the deposition of units ❷ and ❸. Given the range in estimated age for these units (Table 1), this possible rupture would have occurred between AD 230 and 1290. Also, if the upward termination of the fault strand exposed on the southeastern wall of trench 1 (station 6.0 m, Figure 5) reflects a possible rupture between the lower and upper parts of unit ❸, this rupture would have occurred between AD 1190 and 1640 (based on the range in estimated age of unit ❸, Table 1). Lastly, if unit ❻ represents a local fissure filling (rather than merely sheared alluvium), it might record the occurrence of surface rupture between deposition of unit ❺ (undated) and unit ❼ (ca. 1906). In this scenario, the penultimate rupture at the Fort Ross Orchard site would have occurred between AD 1490 (the minimum constraining age for unit ❺, based on dates from unit ❸; Table 1) and AD 1906 (the likely age of unit ❼). Additional charcoal samples taken from unit ❻ could provide a better estimate of deposit age, and would help with the stratigraphic correlation and interpretation of deposit origin, and thus with the past earthquake history. We emphasize that these data are preliminary and speculative, and that additional exposures of faulted deposits and additional age dates are needed to confirm or refute any of these possible events.

Although the speculative interpretations presented above are poorly constrained, the broad time windows are consistent with results from sites to the north and south (see summary in Knudsen et al., 2002). For example, the penultimate earthquake is interpreted to have occurred between AD 1630 and 1906 at Point Arena (Prentice et al., 2000), and between AD 1490 and 1906 at the Fort Ross Orchard site. Similarly, the rupture interpreted by our previous studies at the nearby Archae Camp occurred between AD 1170 and 1650 (Simpson et al., 1996), and we herein provide limited evidence of a rupture between AD 1190 and 1640. Finally, studies at Point Arena (Prentice, 1989; Prentice et al., 2000) identified two additional ruptures between AD 1 and 1310, and work by Simpson et al. (1996) suggest the occurrence of two ruptures between AD 560 and 1290 at the Archae Camp site (Figure 1). The limited data from Fort Ross Orchard suggest a possible rupture within this time period (between AD 230 and 1290). Thus, although the available data from the Fort Ross Orchard site are limited, the results are consistent with other nearby sites on the North Coast segment of the San Andreas Fault.

Our field efforts at the Fort Ross Orchard site also included fault-parallel trenches on both sides of the fault to provide possible stratigraphic constraints on fault slip rate (trenches 2 and 3, Figure 4). Trench 2 was excavated along the crest of the linear ridge west of the fault, across a topographic saddle developed in the ridge. A 1-m-wide sediment-filled paleochannel cut into bedrock underlies this saddle and trends roughly orthogonal to the fault. Age dates from charcoal in this paleochannel suggest an age of AD 1260 to 1390. We excavated trench 3 on the eastern side of the fault to test the hypothesis that the bedrock notch originally was a through-going channel that has been offset and thus could be used as a piercing point to estimate the late Holocene fault slip rate. Unfortunately, a similar channel-shaped feature was not encountered in trench 3 east of the fault, although the sediments in the linear depression east of the fault span this age range. Thus, the available trench exposure did not provide well-constrained information on the fault slip rate during this investigation.

Nevertheless, this field effort provides information that may help limit the late Holocene slip rate on the San Andreas Fault at this site. We question why the paleochannel on the southwestern side of the fault is distinct and well formed, whereas there is no evidence of a similar feature on the northeastern side of the fault. Based on available age estimates, the paleochannel would be expected to be located stratigraphically in the middle of unit ❸, which is continuous throughout trench 3. We consider that either no channel was formed northeast of the fault, or that our studies did not expose the channel. In the first of these two cases, deposition could have occurred within the linear trough until it was filled to the elevation of the crest of the shutter ridge, and then incised into the bedrock southwest of the fault. In this case, coarse clasts would have been deposited into the linear trough and fine-grained alluvial-fan sediments (i.e., unit ❸) would have overtopped the ridge. However, the paleochannel exposed in trench 2 on the southwestern side of the fault contains large, rounded sandstone clasts, which indicate a high-energy, through-going channel transport system, rather than an alluvial-fan depositional system.

In addition, the present-day closed depression at the site shows that the linear trough was not completely filled, and thus that an integrated depositional system did not form after the initial development of the shutter ridge. We interpret that a through-going channel transport system pre-dates development of the linear trough that is present northeast of the shutter ridge at the site.

Therefore, we consider the speculative scenario in which the unit C1 paleochannel is present northeast of the fault but that trench 3 did not extend far enough southeast to encounter it. Based on our detailed field survey of the site, the distance along the fault from the topographic saddle in the ridge crest (which approximates the location of the paleochannel, see Figure 6) to the southeastern end of trench 3 is about 17 m (Figure 4). If the unit C1 paleochannel is farther southeast than the trench 3 exposure, this is a minimum amount of fault offset of the paleochannel. Available radiometric data suggest that the age of the paleochannel is AD 1260 to 1390, and therefore is about 560 to 690 years old. These limited data suggest a minimum late Holocene slip rate of 25 mm/yr.

This estimated slip rate is considerably higher than that provided by recent studies at the nearby Mill Gulch (Prentice et al., 2000, 2001) and Archae Camp sites (Simpson et al., 1996; Noller and Lightfoot, 1997), which indicate a rate of 19 $\pm$ 4 mm/yr. Given this rate, we would expect to find the northeastern equivalent of the unit C1 paleochannel within trench 3. Because we find no viable stratigraphic or geomorphologic explanation for the absence of this paleochannel northeast of the fault, we speculate that perhaps our age estimate is too young, and that perhaps the sample upon which we based our age-estimate was introduced into the deposit following deposition (via burrowing or some other near-surface process). If the paleochannel were actually directly southeast of trench 3 (about 17 m from the topographic saddle), then the slip rate of 19 $\pm$ 4 mm/yr (Prentice et al., 2001) would suggest that unit C1 is about 1,000 years old. If the paleochannel were farther southeast, then the Mill Gulch slip rate would suggest that the paleochannel is older, which is possible given the range in age-dates that were obtained from unit C1 (Table 1). Thus, although the data developed in this study suggests a minimum slip rate of 25 mm/yr for the San Andreas Fault, the uncertainty in deposit age suggests that this minimum rate is not robust.

5.0
CONCLUSIONS

The Fort Ross Orchard site, which lies astride the North Coast segment of the San Andreas Fault, is characterized by a narrow shutter ridge and associated linear trough within which latest Holocene sediments have accumulated. We excavated one trench across the San Andreas Fault and into these alluvial sediments, and one fault-parallel trench northeast of the fault to provide three-dimensional exposures of the alluvium trapped behind the linear shutter ridge. We excavated a third intersecting trench, also parallel to the fault, along the crest of the linear ridge to expose a buried paleochannel that traverses the ridge crest. We interpret that this paleochannel is the southwestern extension of the present-day incised drainage northeast of the fault that is the source of the trapped alluvium.

In general, the trenches show that the alluvial-fan sediments consist of clayey sand deposited against the east-facing fault scarp. These thick-bedded deposits are displaced by the fault and range in age from about AD 230 to AD 1640. In addition, trench 1 shows the presence of scarp-derived colluvium shed into the linear depression from the bedrock-cored shutter ridge. We interpret that the colluvium reflects degradation of the scarp produced in 1906.

Geologic relations exposed in trench 1 at the Fort Ross Orchard site provide possible evidence of three pre-1906 earthquakes, although all of the evidence is equivocal at this time. Beneath the post-1906 colluvium is a sheared deposit that may be either faulted alluvium or an older fissure fill. Stratigraphic relations and age dating suggest that this unit is younger than about AD 1640 (but older than 1906). Two pre-1640 earthquakes are suggested by two upward fault terminations within the lower alluvium, although these terminations occur at different stratigraphic levels. Given available age-estimates, the trench relations suggest possible surface ruptures between AD 230 and 1290, between AD 780 and 1640, and between AD 1640 and 1906. We emphasize that these data are poorly constrained, and that additional exposures of faulted deposits and additional age dates are needed to confirm or refute any of these possible events. Nevertheless, the broad time windows of these possible ruptures are consistent with results from the Point Arena area to the northwest (Prentice et al., 2000) and the nearby Archae Camp site southeast (Simpson et al., 1996). Thus, although the available data from the Fort Ross Orchard site are limited, the results are consistent with other nearby sites on the North Coast segment of the San Andreas Fault.

Our excavations at the Fort Ross Orchard site also included fault-parallel trenches on both sides of the fault to provide possible stratigraphic constraints on fault slip rate. Trench 2 was excavated along the crest of the linear ridge west of the fault, across a topographic saddle developed on the ridge. A 1-m-wide sediment-filled bedrock paleochannel underlies this saddle and trends roughly orthogonal to the fault. Based on multiple age dates from charcoal in this paleochannel, we interpret an age of AD 1260 to 1390 for the deposits filling the paleochannel, although a broad range in age-dates allows the channel to be considerably older. We excavated trench 3 on the eastern side of the fault to test the hypothesis that the paleochannel originally was a through-going channel that has been offset and thus can be used as a piercing point to estimate the late Holocene fault slip rate. Unfortunately, a similar paleochannel was not encountered in the fault-parallel trench northeast of the fault, and the available trench exposures did not provide well-constrained information on the fault slip rate.

Nevertheless, this field effort provides information that may help limit the late Holocene slip rate on the San Andreas Fault at this site. We speculate that trench 3 was not long enough to expose the paleochannel on the northeastern side of the fault. Based on our detailed field survey of the site, the distance along the fault from the paleochannel to the southeastern end of trench 3 is about 17 m, which represents a minimum amount of fault offset of the paleochannel. Available radiometric data suggest that the paleochannel is about 560 to 690 years old, which suggests a minimum late Holocene slip rate of 25 mm/yr. Because this estimated slip rate is considerably higher than the rate of 19 $\pm$ 4 mm/yr obtained by recent studies at the nearby Mill Gulch (Prentice et al., 2000, 2001) and Archae Camp sites (Simpson et al., 1996; Noller and Lightfoot, 1997), and because we find no viable stratigraphic or geomorphologic explanation for the absence of the paleochannel northeast of the fault, we speculate that our age estimate for the paleochannel may be too young. Thus, although the data developed in this study suggests a minimum slip rate of 25 mm/yr for the San Andreas Fault, the uncertainty in deposit age suggests that this rate is not robust.

6.0 ACKNOWLEDGEMENTS

This research was supported by the U.S. Geological Survey (USGS), Department of the Interior, under USGS award number 01-HQ-GR-0072. The views and conclusions contained in this document are those of the authors and should not be interpreted as necessarily representing the official policies, either expressed or implied, of the U.S. Government. Thanks are graciously extended to Park Rangers Bill Walton and Dan Murley of Fort Ross State Historic Park, and to Heidi Horvitz (Supervising Ranger) and Breck Parkman (Regional Archaeologist) with the California Department of Parks and Recreation, for making this project happen. Thanks also to Carol Prentice, Tom Fumal, David Schwartz, Chris Crosby, Heidi Stenner, and Tim Dawson (U.S. Geological Survey), Koji Okimura (Hiroshima University), Rich Briggs (Center for Neotectonics Studies, Reno), and Omer Emre (Turkish Mineral Research and Exploration) for providing insightful field discussions. Our appreciation also goes to Gordon Seitz and John Southon (Center for Accelerator Mass Spectrometry, Lawrence Livermore National Laboratories) for completing the radiometric analyses, under the USGS Bay Area Paleoseismological Experiment (BAPEX) program.

7.0
REFERENCES

Baldwin, J.N., 1996, Paleoseismic investigation of the San Andreas fault on the north coast segment, near Manchester, California: M.S. thesis San Jose State University, 127 p. plus plates.

Baldwin, J.N., Knudsen, K.L., Lee, A., Prentice, C.S., and Gross, R., 2000, Preliminary estimate of coseismic displacement of the penultimate earthquake on the northern San Andreas Fault, Pt. Arena, California: *in* Bokelman, G., and Kovachs, R., eds., Tectonic problems of the San Andreas fault system, Stanford University Publications, p. 355-368.

Brown, R.D., and Wolfe, E.W., 1970, Map showing recently active breaks along the San Andreas fault between Point Delgada and Bolinas Bay, California: U.S. Geological Survey Miscellaneous Field Investigations Map I-692, scale 1:24,000.

Fumal, T.E., Heingartner, G.F., and Schwartz, D.P., 1999, Timing and slip of large earthquakes on the San Andreas fault, Santa Cruz Mountains, California [abs.]: Geological Society of America Abstracts with Programs, v. 31, no. 6, p. A-56.

Hall, N.T., Wright, R. H., and Clahan, K. B., 1999, Paleoseismic studies of the San Francisco Peninsula segment of the San Andreas fault zone near Woodside, California: Journal of Geophysical Research, v. 104, no. B10, p. 23,215-23,236.

Hill, D.P., Eaton, J.P, and Jones, L.M., 1990, Seismicity, 1980-1986, in Wallace, R.E., ed., The San Andreas Fault System, California: U.S. Geological Survey Professional Paper 1515, p. 115-151.

Kelson, K.I., and Lettis, W.R., 2001, Evaluation of paleoearthquakes along the northern San Andreas Fault, Fort Ross State Historic Park, California: Annual Summary submitted to the U.S. Geologic Survey National Earthquake Hazard Reduction Program <http://erp-web.er.usgs.gov/reports/annsum/vol42/nc/nc_vol42.htm>.

Knudsen, K.L., Witter, R.C., Garrison-Laney, C.E., Baldwin, J.N., and Carver, G.A, 2002, Past earthquake-induced rapid subsidence along the northern San Andreas fault: A paleoseismological method for investigating strike-slip faults: Bulletin of the Seismological Society of America, v. 92, no. 7, p. 2612-2636.

Lawson, A.C., 1908, The California earthquake of April 18, 1906: Report of the State Earthquake Investigation Commission (Reprinted 1969), v. 1, Carnegie Institution of Washington Publication, 451 p. and atlas.

Muhs, D.R., Prentice, C., and Merritts, D.J., 2003, Marine terraces, sea level history, and Quaternary tectonics of the San Andreas fault on the coast of California: *in* Easterbrook, D., ed., Quaternary Geology of the United States, INQUA 2003 Field Guide Volume, Desert Research Institute, Reno, NV, p. 1-18.

Niemi, T.M., and Hall, N.T., 1992, Late Holocene slip rate and recurrence of great earthquakes on the San Andreas fault in northern California: Geology, v. 20, p. 195-198.

Niemi, T.M., Zhang, H., Generaux, S., Fumal, T. and Seitz, G., 2002, A 2500-year record of earthquakes along the northern San Andreas fault at Vedanta Marsh, Olema, CA[abs]: Geological Society of America Cordilleran Section, 98th Annual Meeting Abstracts With Programs, v. 34, no. 5, p. 86.

Noller, J.S., Kelson, K.I., Lettis, W.R., Wickens, K.A., Simpson, G.D., Lightfoot, K., Wake, T., 1993, Preliminary characterizations of Holocene activity on the San Andreas fault based on offset archaeological sites, Ft. Ross State Historic Park, California: NEHRP Final Technical Report.

Noller, J.S., and Lightfoot, K.G., 1997, An archaeoseismic approach and method for the study of active strike-slip faults: Geoarchaeology: An International Journal, v. 12, p. 117-135.

Prentice, C.S., 1989, Earthquake geology of the northern San Andreas Fault near Point Arena, California: Pasadena, California, California Institute of Technology, Ph.D. Dissertation, 252 p.

Prentice, C.S., Langridge, R., and Merritts, D.J., 2000, Paleoseismic and Quaternary tectonic studies of the San Andreas fault from Shelter Cove to Fort Ross: *in* Bokelman, G., and Kovachs, R. eds., Tectonic problems of the San Andreas fault system, Stanford University Publications, p. 349-351.

Prentice, C.S., Prescott, W.H., and Langridge, R., 2001, New geologic and geodetic slip rate estimates on the North Coast San Andreas Fault: Approaching agreement? [abs]: Seismological Research Letters, v. 72, no. 2, p. 282.

Prentice, C.S., Merritts, D.J., Beutner, E.C., Bodin, P., Schill, A., and Muller, J.R., 1999, Northern San Andreas fault near Shelter Cove, California: Geological Society of America Bulletin, v. 111, no. 4, p. 512-523.

Schwartz, D.P., Pantosti, D., Okumura, K., Powers, T.J., and Hamilton, J.C., 1998, Paleoseismic investigations in the Santa Cruz Mountains, California: Implications for recurrence of large-magnitude earthquakes on the San Andreas fault: Journal of Geophysical Research, v. 103, p. 17,985-18,001.

Simpson, G.D., Noller, J.S., Kelson, K.I., and Lettis, W.R., 1996, Logs of trenches across the San Andreas fault, Archae camp, Fort Ross State Historic Park, Northern California: U.S. Geological Survey NEHRP Final Technical Report

Stuiver, M., and Reimer, P.J., 1993, Extended ^{14}C data base and revised CALIB 3.0 ^{14}C age calibration program: Radiocarbon, v. 35, p. 215-230.

Stuiver, M., and Reimer, P.J., 2000, CALIB v4.3 ^{14}C age calibration program.

Thatcher, W., Marshall, G., and Lisowski, M., 1997, Resolution of fault slip along the 470-km-long rupture of the great 1906 San Francisco earthquake and its implications: Journal of Geophysical Research, v. 102, no. B3, p. 5353-5367.

Toppozada, T.R., Reel, C.R., and Parke, D.L., 1981, Preparation of isoseismal maps and summaries of reported effects for pre-1990 California earthquakes: California Division of Mines and Geology Open-File Report 81-11, 182 p.

Wagner, D.L., and Bortugno, E.J., 1982, Geologic Map of the Santa Rosa Quadrangle, California: California Division of Mines and Geology, Regional Geologic Map Series, Santa Rosa Quadrangle, Map 2A (Geology), Sheet 1 of 5, scale 1:250,000.

Working Group on California Earthquake Probabilities (WGCEP), 1990, Probabilities of large earthquakes in the San Francisco Bay region, California: U.S. Geological Survey Circ. 1053, 51p.

Working Group on California Earthquake Probabilities (WGCEP), 1999, Probabilities of large earthquakes in the San Francisco Bay region, California: U.S. Geological Survey Open-file Report 99-517.

Working Group on California Earthquake Probabilities (WGCEP), 2003, Earthquake probabilities in the San Francisco Bay region: 2002 to 2031--A summary of findings: U.S. Geological Survey Open-file Report 03-214.